

Supplemental Information titles and legends

Supplemental Figures titles and legends

Figure S1.

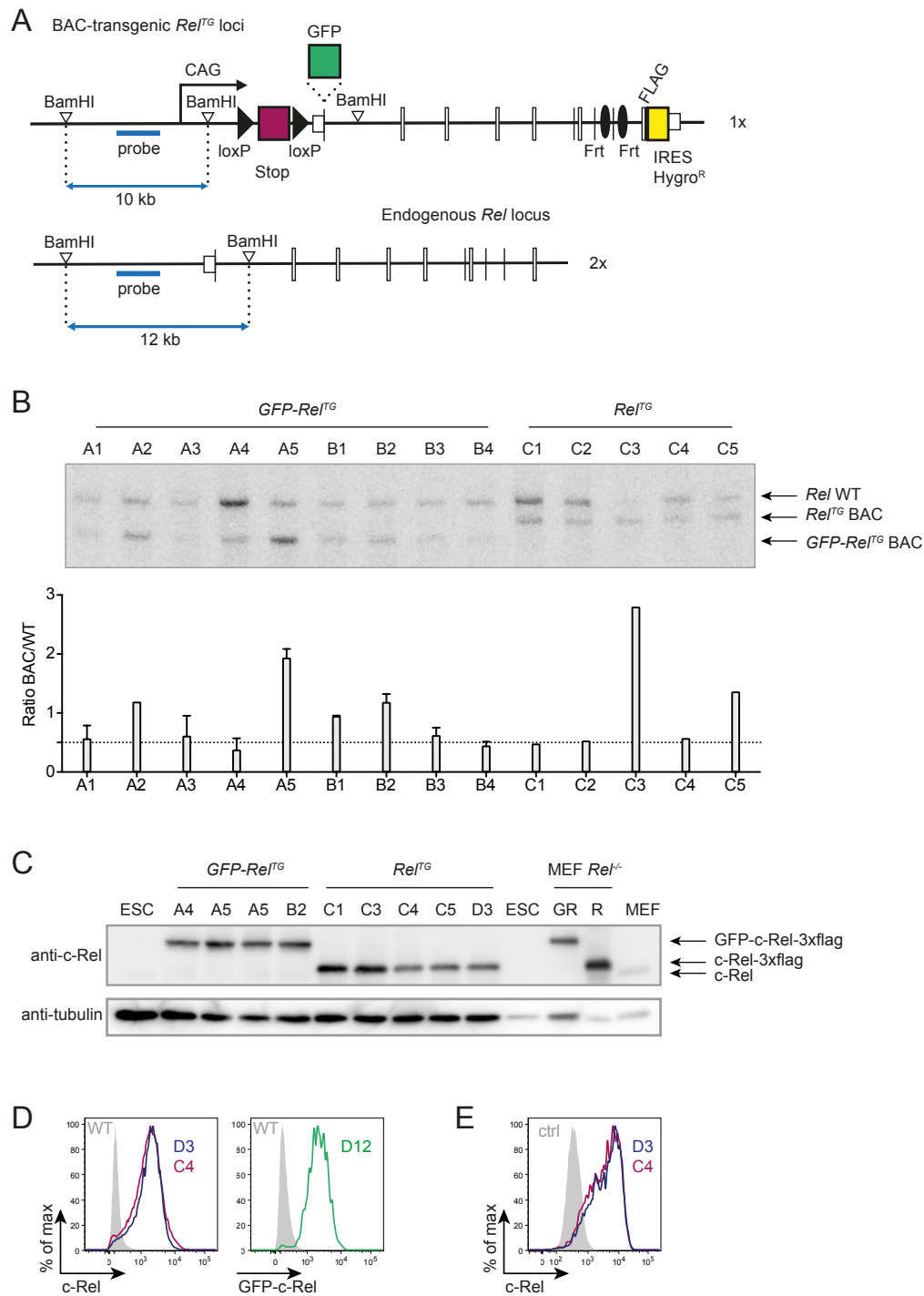


Figure S1. Generation of novel c-Rel transgenic mouse models. Related to Figure 1.

(A) Detailed schematic representation of modified BAC construct for generation of c-Rel transgenic mouse models and endogenous *Rel* locus. Localization of the Southern blot probe and BamHI enzymatic restriction sites resulting in differential fragment sizes for endogenous and modified *Rel* locus to allow quantification of integrants are highlighted (see also method details).

(B) Representative Southern blot of embryonic stem (ES) cell clones of *GFP-Rel^{TG}* and *Rel^{TG}* and quantification of number of transgenic integrants. Clones with single BAC integrants have a ratio of BAC/WT of 0.5 (dotted line). Represented data are quantified from two blots (clones A, B; bars represent mean±SD) or one blot (clones C, bars represent value).

(C-D) Following antibiotic selection for BAC integration (G418 resistance in stop cassette), ES cell clones were transduced with Cre recombinase and selected for locus expression (hygromycin B selection). c-Rel and GFP-c-Rel protein expression was validated in selected ES cell clones by Western blot (C) and flow cytometry (D). *Rel^{-/-}* MEFs carrying the c-Rel (R)/GFP-c-Rel (GR) BAC and WT MEFs as well as WT ES cells (ESC) served as controls.

(E) Tailtip fibroblasts of transgenic mice were in vitro transduced with Cre recombinase and analyzed for c-Rel expression by intracellular flow cytometry. Untransduced cells served as a control (ctrl).

BAC, bacterial artificial chromosome; Hygro^R, hygromycin B resistance; MEF, mouse embryonic fibroblasts; WT, wild type.

Figure S2.

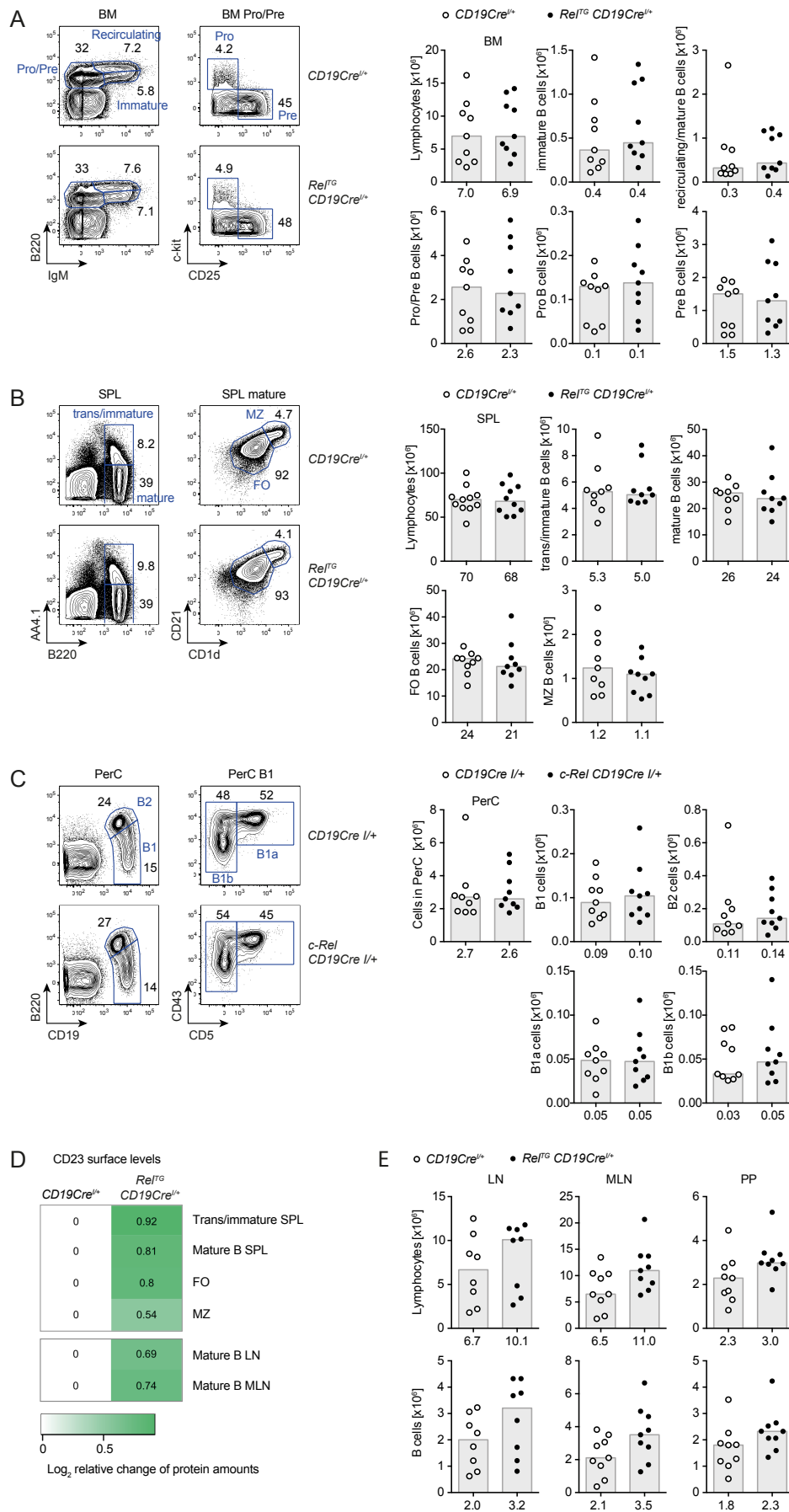


Figure S2. General B cell populations are largely unchanged in *Rel^{TG} CD19Cre^{l/+}* mice.

Related to Figure 1.

(A) Representative flow cytometry plots displaying median percentages of indicated B cell populations in bone marrow (BM). In graphs showing respective cell numbers, individual data points obtained in ≥ 3 independent experiments are plotted. Bars and numbers below graphs are median values. Pro/Pre B220⁺IgM⁻; Pro B220⁺IgM⁻CD25⁻c-kit⁺; Pre B220⁺IgM⁻CD25⁺c-kit⁺; immature B220^{lo}IgM⁺; recirculating/mature B220^{hi}IgM⁺.

(B) Representative flow cytometry plots displaying median percentages of indicated B cell populations in spleen (SPL). In graphs showing respective cell numbers, individual data points obtained in ≥ 3 independent experiments are plotted. Bars and numbers below graphs are median values. Transitional/immature B220⁺AA4.1⁺; mature B220⁺AA4.1⁺; follicular (FO) B220⁺AA4.1⁻CD1d^{int}CD21^{int}; marginal zone (MZ) B220⁺AA4.1⁻CD1d^{hi}CD21^{hi}.

(C) Representative flow cytometry plots displaying median percentages of indicated B cell populations in peritoneal cavity (PerC). In graphs showing respective cell numbers, individual data points obtained in 3 independent experiments are plotted. Bars and numbers below graphs are median values. PerC B2 CD19⁺B220^{high}; PerC B1 CD19⁺B220^{low}; PerC B1a CD43⁺CD5⁺; PerC B1b CD43^{low}CD5⁻.

(D) Heatmap representation of CD23 surface level expression assessed by flow cytometry.

CD23 median fluorescence intensities were normalized to *CD19Cre^{l/+}* controls in each subpopulation and log₂ fold change values of geometric means are displayed. Data were obtained in ≥ 3 independent experiments and are representative for 5-9 mice per genotype.

Gating of B cell populations as defined in (B).

(E) Lymphocyte and B cell numbers in indicated organs. Individual data points obtained in ≥ 3 independent experiments are plotted. Bars and numbers below graphs are median values.

LN, lymph nodes; MLN, mesenteric lymph nodes; PP, Peyer's patches.

Figure S3.

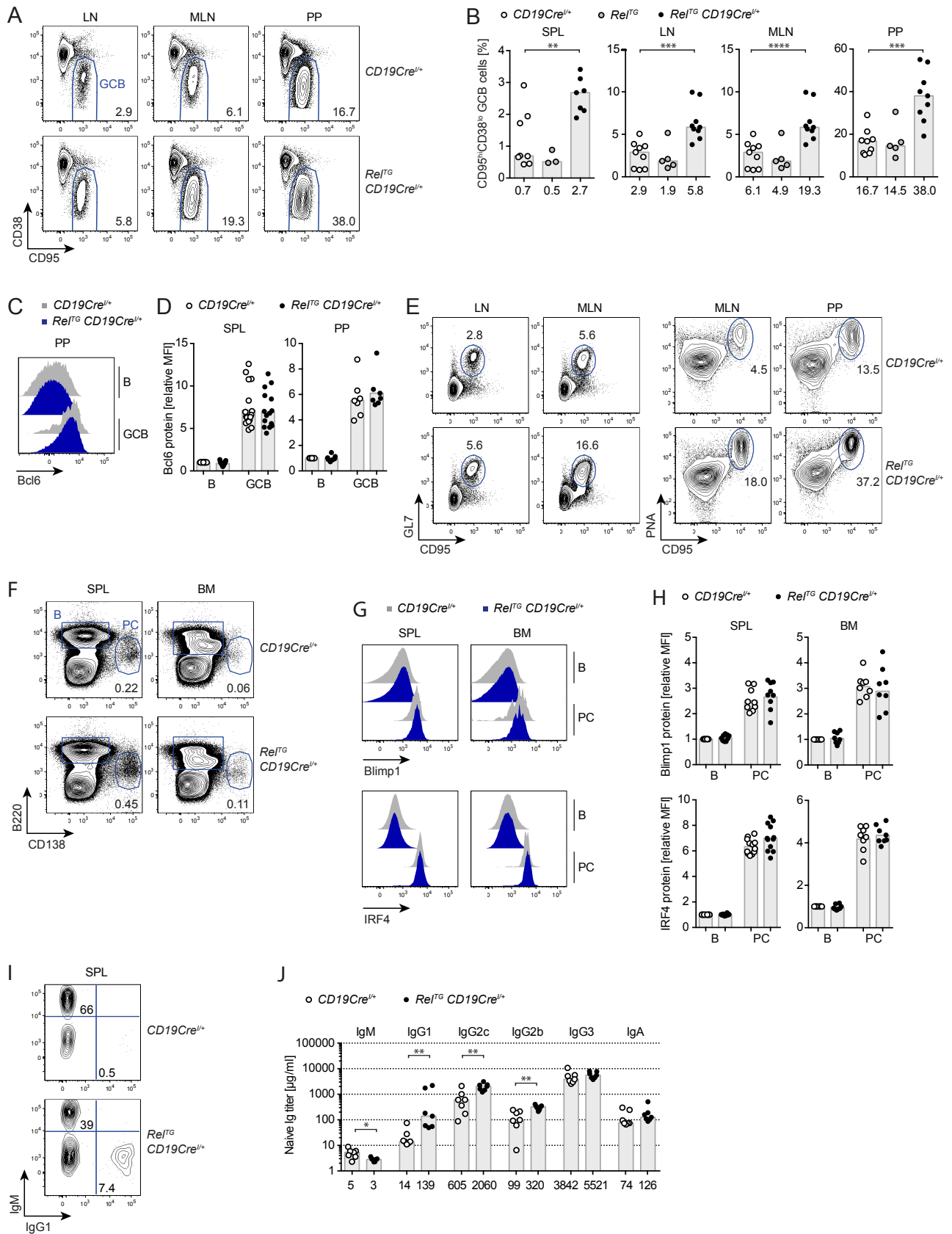


Figure S3. GCB cell and plasma cell population percentages, expression of markers and serum Ig subtype titers. Related to Figure 1.

(A) Representative flow cytometry plots of GCB cells (B220⁺/CD19⁺ CD95^{hi}CD38^{lo}). Displayed numbers are median percentages of GCB cells within the population of B cells (n ≥ 8).

(B) Percentages of GCB cells. Individual data points obtained in ≥ 3 independent experiments are plotted. Bars and numbers below graphs are median values. **p ≤ 0.01, ***p ≤ 0.001, ****p ≤ 0.0001, one-way ANOVA.

(C) Representative flow cytometry histograms of intracellular Bcl6 protein expression.

(D) Intracellular Bcl6 expression determined by flow cytometry. MFIs are normalized to the non-GCB cell population of *CD19Cre^{l/+}* controls. Individual data points obtained in ≥ 3 independent experiments and bars representing geometric means are plotted.

(E) Representative flow cytometry plots of additional GCB cell marker expression. Numbers are percentages of shown example plots.

(F) Representative flow cytometry plots of plasma cells (B220^{lo}CD138⁺). Displayed numbers are median percentages (n ≥ 12).

(G) Representative flow cytometry histograms of intracellular Blimp1 and IRF4 expression.

(H) Intracellular Blimp1 and IRF4 expression in plasma cells determined by flow cytometry. MFIs are normalized to the B cell population of *CD19Cre^{l/+}* controls. Individual data points obtained in ≥ 3 independent experiments and bars representing geometric means are plotted.

(I) Representative flow cytometry plots of intracellular Ig subtype staining in plasma cells (n ≥ 8).

(J) Naïve serum titers of indicated Ig isotypes measured by ELISA. Individual data points are plotted (n = 7). Bars and numbers below graphs are median values. Serum was collected in independent experiments. *p ≤ 0.05, **p ≤ 0.01, Mann-Whitney test.

SPL, spleen; LN, lymph nodes; MLN, mesenteric lymph nodes; PP, Peyer's patches; BM, bone marrow; MFI, median fluorescence intensity.

Figure S4.

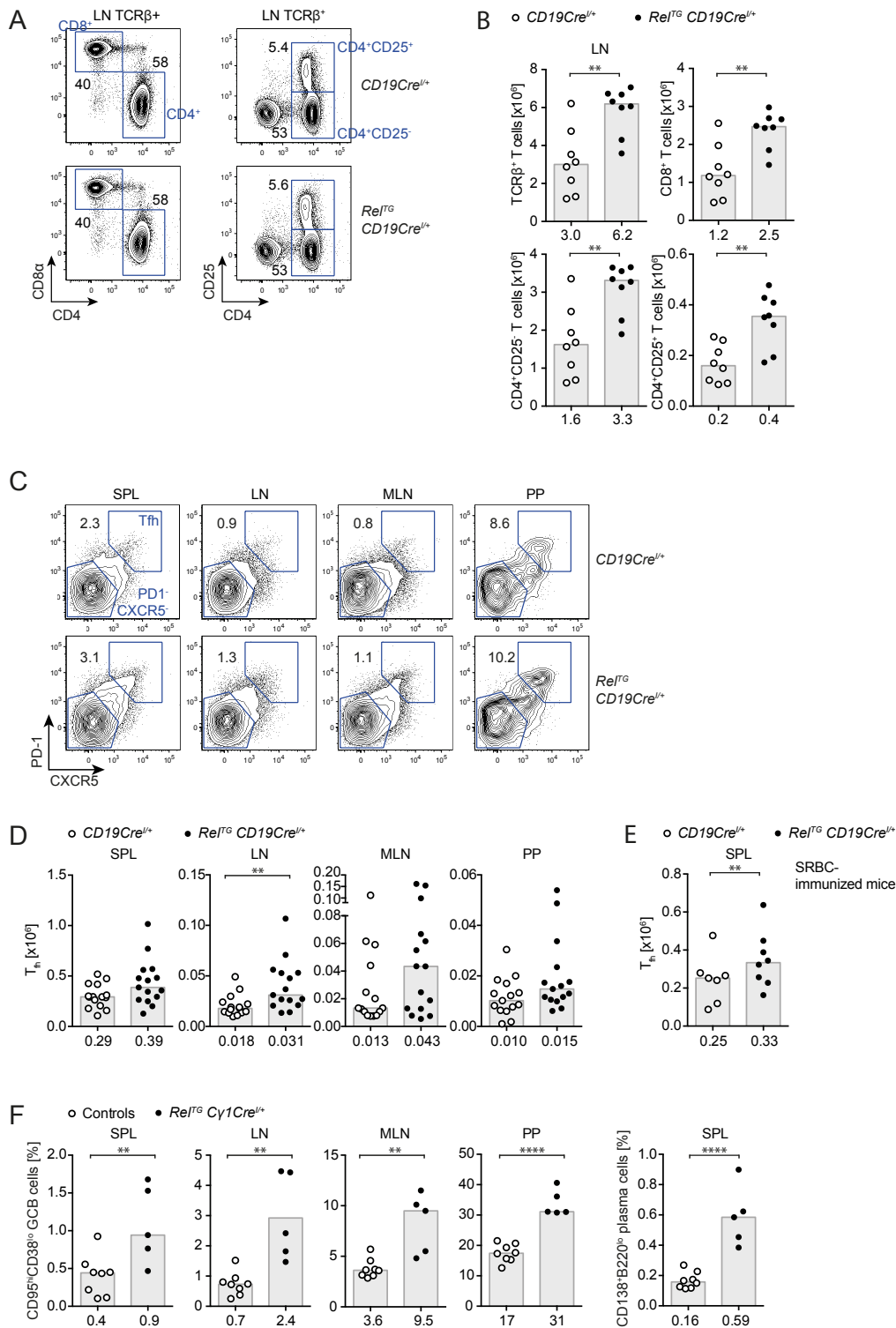


Figure S4. Expansion of GCB cells upon B cell specific c-Rel transgene expression is accompanied by expansion of Tfh cells. Related to Figures 1, 2 and 3.

(A) Representative flow cytometry plots of T cell populations in lymph nodes. Displayed numbers are median percentages (n = 8).

(B) Cell numbers of T cell subpopulations in lymph nodes. Individual data points obtained in 3 independent experiments are plotted. Bars and numbers below graphs represent median values. ** $p \leq 0.01$, unpaired t test.

(C) Representative flow cytometry plots of T_{fh} cells. Displayed numbers are median percentages (n = 15).

(D) Cell numbers of T_{fh} cells. Individual data points obtained in 6 independent experiments are plotted. Bars and numbers below graphs are median values. ** $p \leq 0.01$, unpaired t test.

(E) Cell numbers of T_{fh} cells in SRBC-immunized mice. Individual data points obtained in 3 independent experiments are plotted. Bars and numbers below graphs are median values. ** $p \leq 0.01$, paired t test.

(F) Percentages of GCB cells and plasma cells in *Rel^{TG} C γ 1Cre^{l/+}* and control mice. Individual data points from 2 independent experiments are plotted. Bars and numbers below graphs are median values. ** $p \leq 0.01$, **** $p \leq 0.0001$, unpaired t test.

SPL, spleen; LN, lymph nodes; MLN, mesenteric lymph nodes; PP, Peyer's patches.

Figure S5.

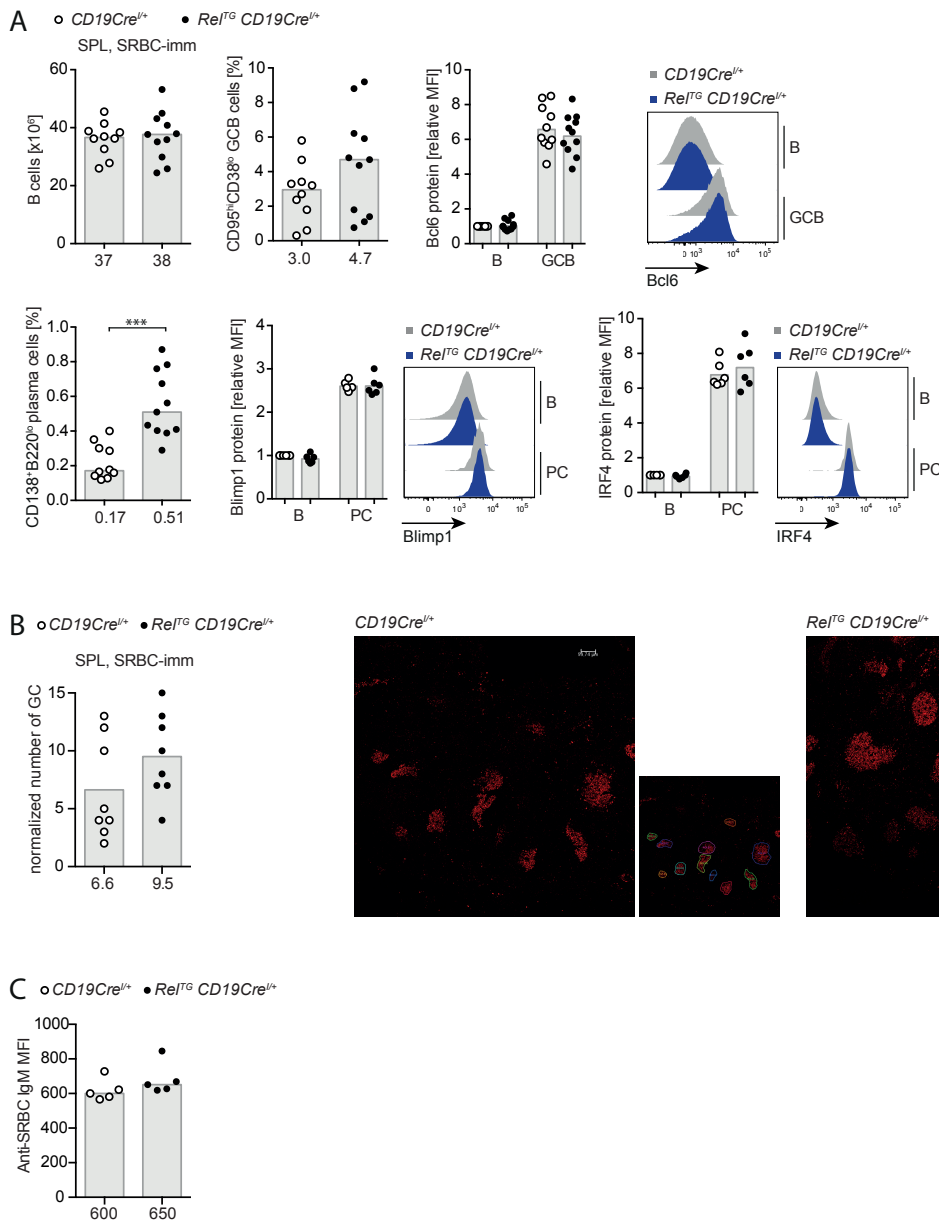


Figure S5. Analysis of GCB and plasma cell expansion in c-Rel transgene-expressing mice upon immunization with SRBC. Related to Figure 2.

(A) Mice were immunized i.p. with SRBC and analyzed 10-12 days post-immunization.

Individual data points obtained in ≥ 2 independent experiments are plotted. For cell numbers and percentages bars and numbers below graphs are median values. *** $p \leq 0.001$, paired t test. For intracellular expression of Bcl6 in GCB cells and Blimp1 and IRF4 in plasma cells

MFIs are normalized to the non-GCB cell population or B cell population of *CD19Cre^{l/+}* controls, respectively, and bars represent geometric means.

(B) Individual data points of the number of splenic GCs normalized to the section area quantified based on Bcl6 immunofluorescence staining 10 days post-immunization (n = 8).

Bars and numbers below bars represent mean values. Representative images of Bcl6 staining are shown. Scale bar: 100 μ m.

(C) Anti-SRBC IgM titer analyzed by flow cytometry 10 days post-immunization. Individual data points of 2 independent experiments are plotted and bars and numbers below graphs are median values.

SPL, spleen; SRBC-imm, SRBC-immunized; MFI, median fluorescence intensities.

Figure S6.

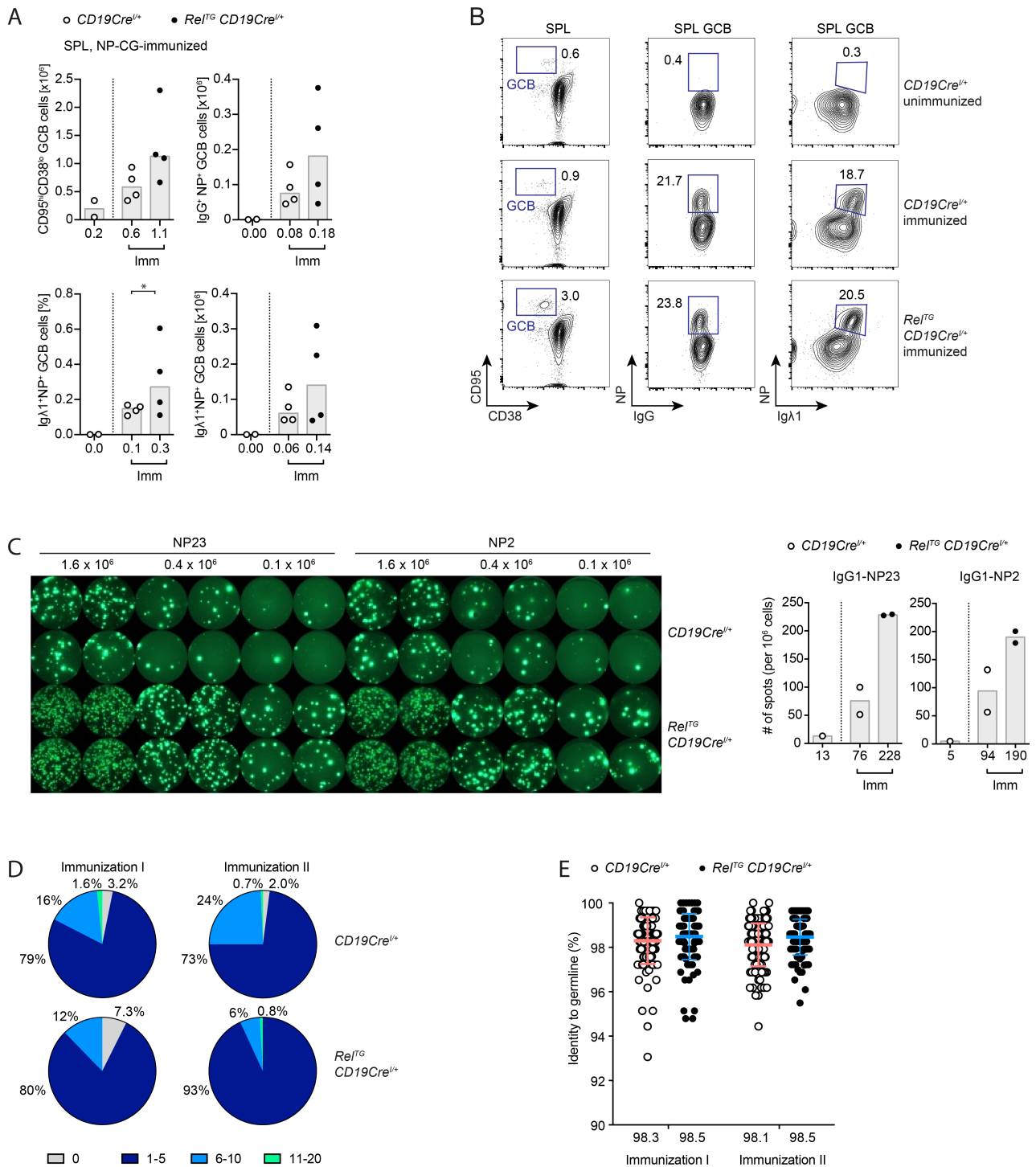


Figure S6. Analysis of GCB and plasma cell expansion as well as somatic hypermutation and affinity maturation in c-Rel transgene-expressing mice upon immunization with NP-CG. Related to Figure 2.

(A) Individual data points for percentage of Igλ1⁺NP⁺ GCB cells within total splenic B cell population and cell numbers for indicated splenic GCB cell populations analyzed 14 days post-NP-CG-immunization are plotted. Bars and numbers below graphs are median values.

(B) Representative flow cytometry plots of unimmunized and NP-CG-immunized mice (n = 4). Numbers are percentages of displayed representative plots.

(C) Anti-IgG1-NP2 and -NP23 FluoroSpot assay analysis 14 days post-immunization with NP-CG. Three different cell numbers for each of 2 mice per genotype were analyzed. For quantification the data for 1.6 x 10⁶ and 0.4 x 10⁶ was normalized to 1 x 10⁶ cells and mean values are displayed for each mouse. Bars and numbers below graphs represent median values.

(D-E) Analysis of somatic hypermutation and affinity maturation in *Rel^{TG} CD19Cre^{l/+}* and *CD19Cre^{l/+}* mice 14 days after immunization with NP-CG. GCB cell VDJ sequencing of IgG1 VH186.2 for 2 independently immunized cohorts with 2 mice per genotype for each cohort. 4 mice *CD19Cre^{l/+}*: immunization I n=126, immunization II n=148; 4 mice *Rel^{TG} CD19Cre^{l/+}*: immunization I n=122, immunization II n=117.

(D) Number of amino acid mutations in VH186.2 presented in groups as percentage of total analyzed data set.

(E) Percentage of V gene identity to germline. Individual data points are plotted. Lines and numbers below graphs represent mean values.

SPL, spleen; imm, immunized.

Figure S7.

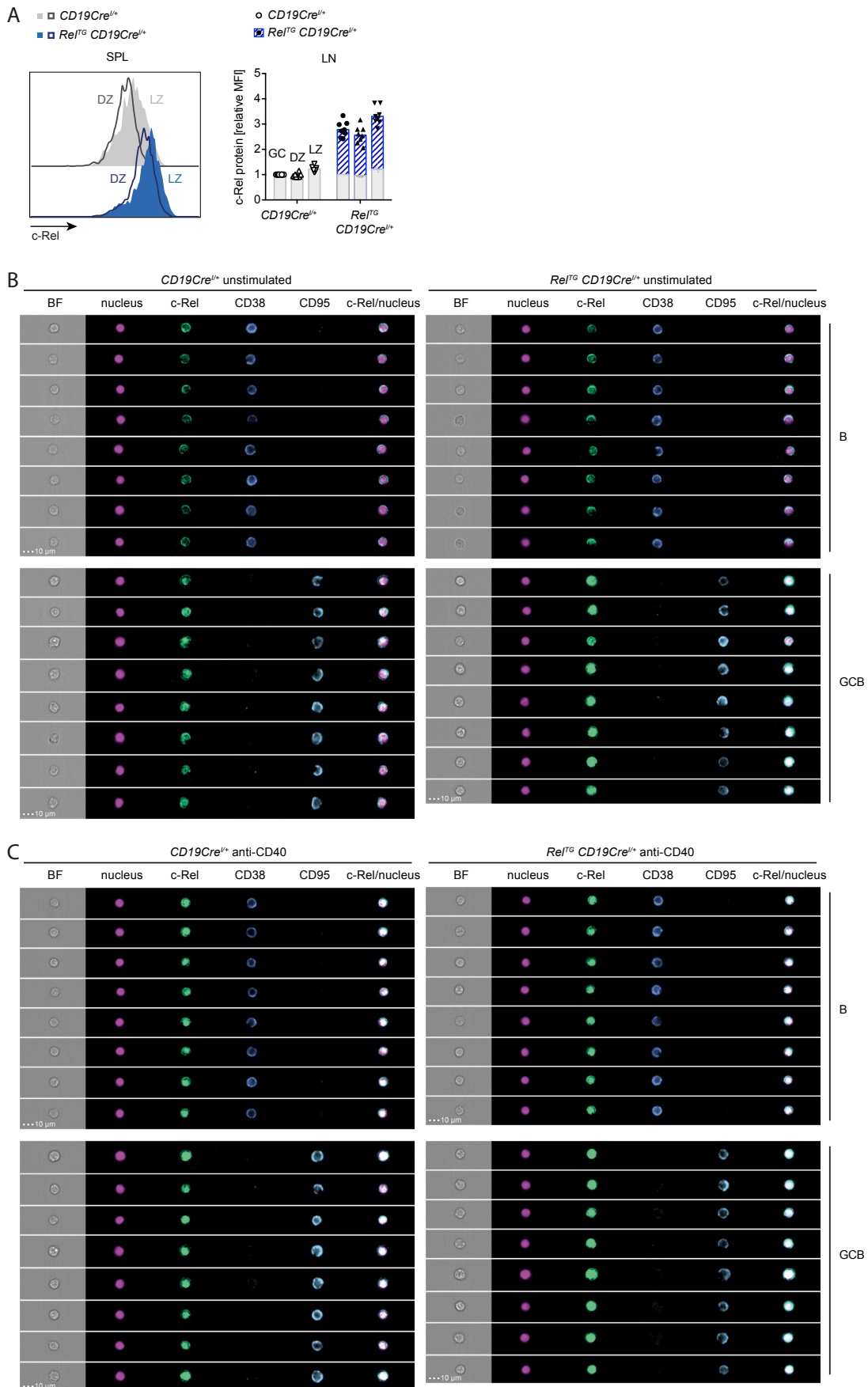


Figure S7. Intracellular c-Rel staining in DZ/LZ GCB cells and imaging flow cytometry example image panels. Related to Figures 5 and 6.

(A) Intracellular flow cytometry data of c-Rel protein abundance in DZ (CXCR4^{hi}CD86^{lo}) and LZ (CXCR4^{lo}CD86^{hi}) cells of the GC normalized to GCB cells of *CD19Cre^{l/+}* controls.

Representative flow cytometry histograms and relative median fluorescence intensities (MFI) of intracellular c-Rel. Individual data points of ≥ 3 independent experiments are plotted. Bars and numbers below graphs are geometric means. The c-Rel protein fraction that is additionally present in c-Rel transgenic mice in comparison to respective control populations is highlighted in blue.

(B-C) Imaging flow cytometry panels for indicated channels of magnified c-Rel/nucleus overlay images shown in Figure 6 for unstimulated cells (C) (including example panels already shown in Figure 6) and anti-CD40 stimulated cells (D) for B cells and GCB cells in lymph nodes from *Rel^{TG} CD19Cre^{l/+}* and *CD19Cre^{l/+}* mice. Scale bar: 10 μ m.

SPL, spleen; LN, lymph nodes.

Figure S8.

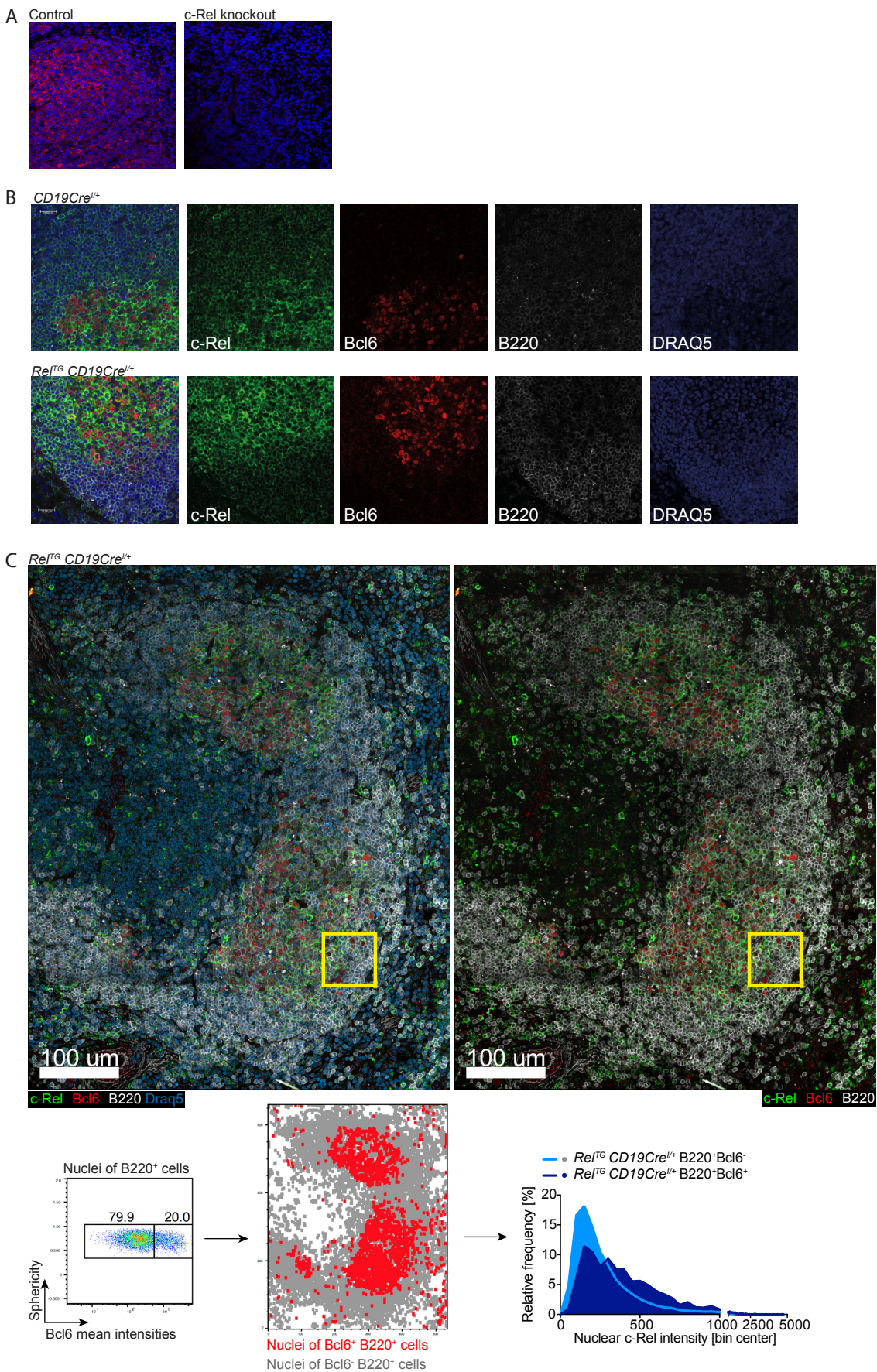


Figure S8. Analysis of c-Rel nuclear translocation by immunofluorescence microscopy.

Related to Figure 7.

(A) Verification of c-Rel antibodies (AF2699, R&D) used: spleen sections of a c-Rel knockout mouse and a control mouse were stained with polyclonal anti-c-Rel antibodies (red) and DAPI (dark blue).

(B) Individual images of the immunofluorescence picture shown in Figure 7A. Scale bar: 20 μm .

(C) Quantification of nuclear c-Rel in splenic B220⁺ cells in *Rel^{TG} CD19Cre^{l/+}* mice by histocytometry. Overview image (c-Rel: green, Bcl6: red, B220: white, Draq5: blue) and analysis for an exemplary/representative confocal image is shown. Inserts show region of interest depicted in Figure 7B. Histocytometry gating, projection onto the section and intensities of reconstructed surface objects for individual nuclei of B220⁺Bcl6⁻ cells (n = 5980) and B220⁺Bcl6⁺ cells (n = 1767) are displayed. Scale bar: 100 μm .

Figure S9.

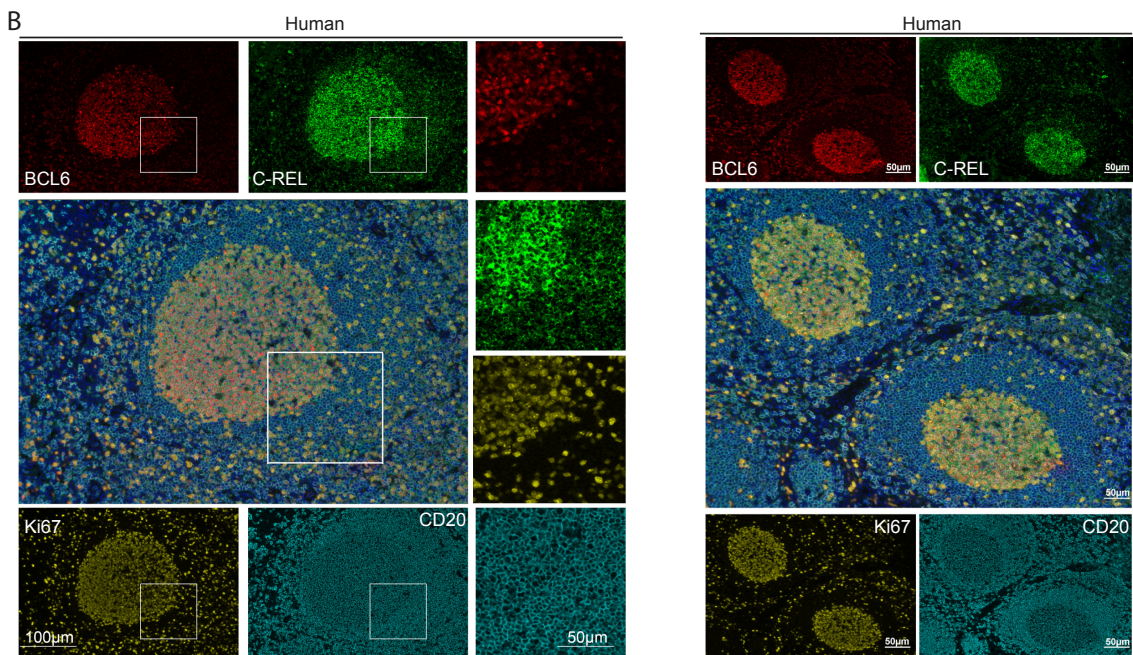
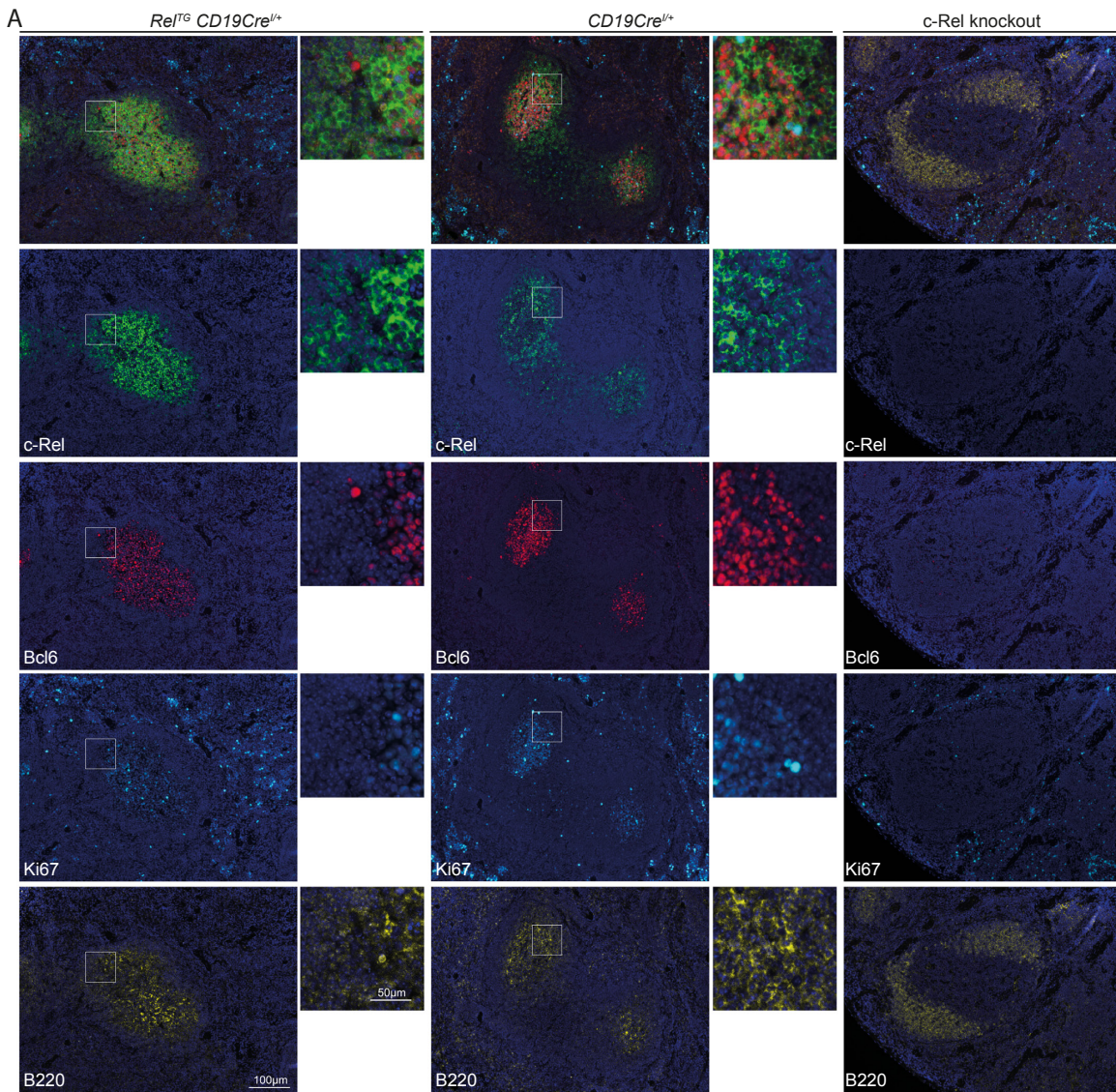


Figure S9. Immunofluorescence of c-Rel nuclear translocation. Related to Figure 7.

(A) Nuclear c-Rel expression assessed by immunohistochemistry example images. Full exemplary image panel for example images shown in Figure 7C for *Rel^{TG} CD19Cre^{l/+}*, *CD19Cre^{l/+}* and c-Rel knockout control are shown (c-Rel: green, Bcl6: red, B220: yellow, Ki67: light blue, DAPI: dark blue). c-Rel knockout serves to validate the polyclonal c-Rel antibodies used here (#4727, Cell Signaling). Scale bar full images: 100 μ m, scale bar section of interest: 50 μ m.

(B) Full exemplary image panels for example images shown in main Figure 7D for staining in human tonsils are shown (left panels, scale bar full images: 100 μ m, scale bar section of interest: 50 μ m), as well as additional tonsil staining (right panels, scale bar: 50 μ m) (c-Rel: green, Bcl6: red, CD20: blue, Ki67: yellow, DAPI: dark blue).

Figure S10.

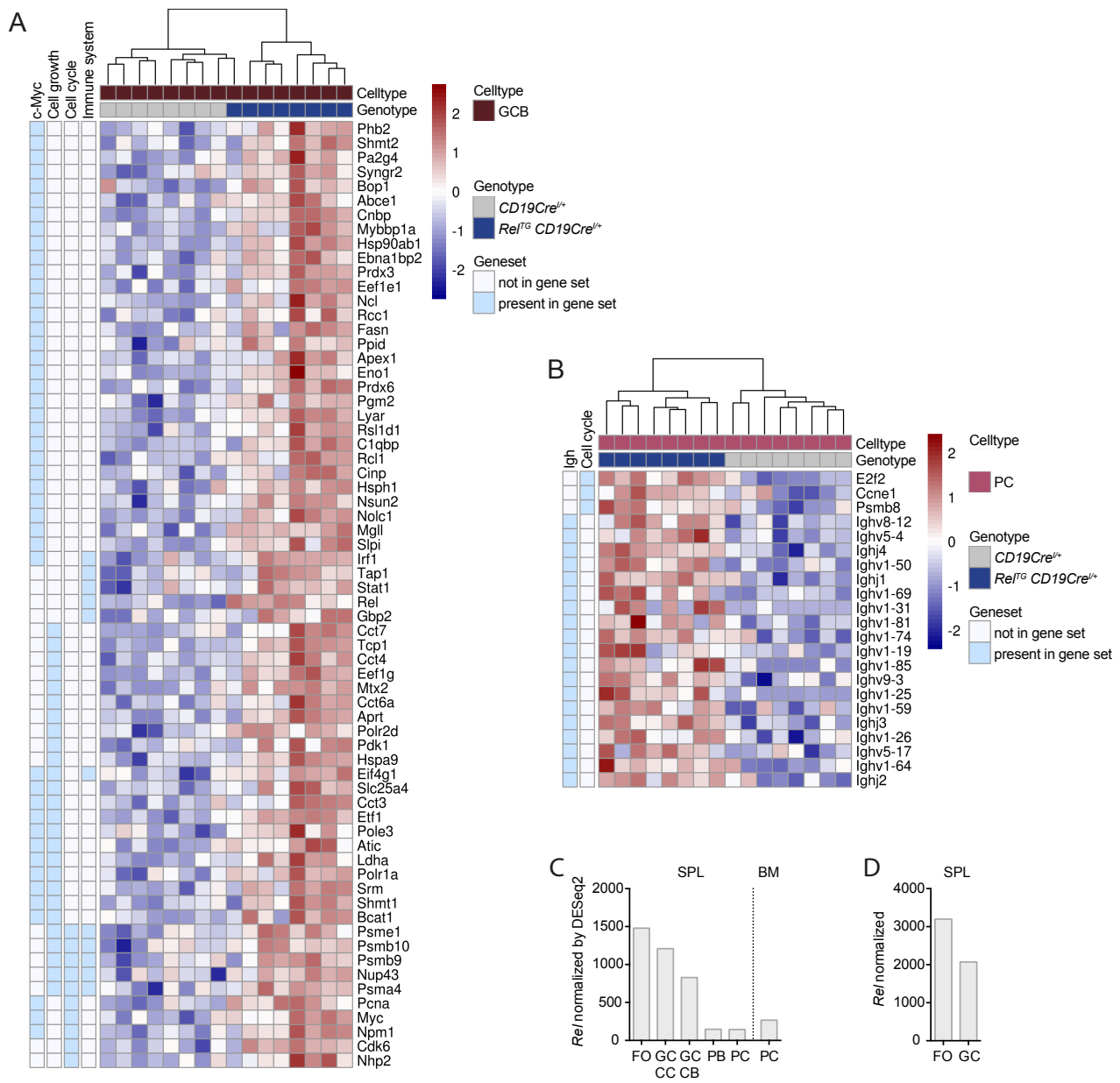


Figure S10. Additional data for RNA sequencing results. Related to Figure 8.

(A) Significantly expressed genes (padj < 0.05; FC ≥ 1.2) amongst the leading edge genes extracted from all gene sets of the categories cell cycle, cell growth/metabolism, immune system (C2: CP) as well as the c-Myc-signatures (MYC C2) that were significantly positively enriched by GSEA in transgenic GCB cells. z-transformed expression values for each of 8 individual mice per genotype are shown in a heatmap representation.

(B) Significantly expressed genes ($p_{adj} < 0.05$; $FC \geq 1.3$) amongst the leading edge genes extracted from cell cycle associated gene sets (C2: CP) that were significantly positively enriched by GSEA in transgenic plasma cells as well as Igh genes. z-transformed expression values for each of 8 individual mice per genotype are shown in a heatmap representation.

(C-D) Data extracted from the Immunological Genome Project (ImmGen) consortium (Heng TSP, Painter MW, Immunological Genome Project Consortium. The Immunological Genome Project: networks of gene expression in immune cells. Nat Immunol. 2008;9(10):1091–1094.) gene skyline dataset for the gene symbol *Rel*. (C) RNA sequencing data expression values normalized by DESeq2 for populations B.Fo.Sp (SPL: FO), B.GC.CC.Sp (SPL: GC CC), B.GC.CB.Sp (SPL: GC CB), P.PB.Sp (SPL: PB), P.PC.Sp (SPL: PC), P.PC.BM (BM: PC) (D) Microarray data based on ImmGen data set GSE15907 normalized data for populations B.Fo.Sp (SPL: FO) and B.GC.Sp (SPL: GC).

Figure S11.

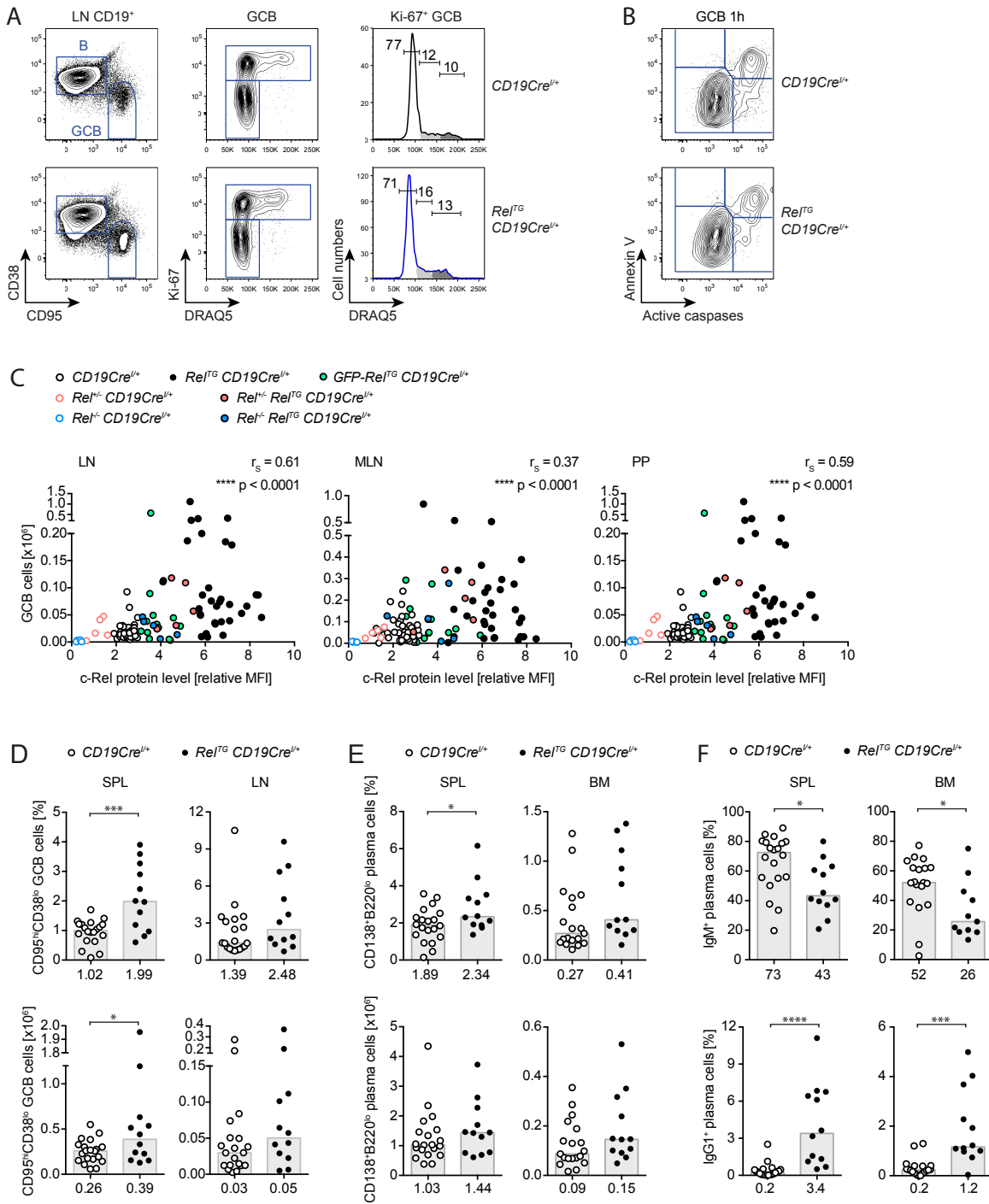


Figure S11. Functional consequences of c-Rel overexpression in young and aged mice.

Related to Figures 9 and 10.

(A) Representative histograms showing gating strategy for cell cycle analysis in GCB cells ($CD19^+CD95^{hi}CD38^{lo}$). Displayed numbers are mean percentages.

(B) Representative flow cytometry plots showing gating strategy for assessment of apoptosis for data shown in Figure 9B.

(C) Correlation of c-Rel protein levels with cellular expansion. The Spearman correlation coefficient and p-values are given. c-Rel protein levels are normalized to non-GCB cells of *CD19Cre^{l/+}* mice. GCB ($CD19^+/B220^+CD95^{hi}CD38^{lo}$): $n_{LN} = 107$; $n_{MLN} = 108$; $n_{PP} = 89$.

(D-F) Percentages and cell numbers of (D) GCB cells and (E) plasma cells as well as (F) percentage of IgM- and IgG1-expressing plasma cells in aged mice. Individual data points obtained in 8 independent experiments from mice aged 409-571 days (median *CD19Cre^{l/+}*: 522 days; median *Rel^{TG} CD19Cre^{l/+}*: 511 days) are plotted. Bars and numbers below graphs are median values. * $p \leq 0.05$, *** $p \leq 0.001$, **** $p \leq 0.0001$, unpaired t test.

SPL, spleen; LN, lymph nodes; MLN, mesenteric lymph nodes; PP, Peyer's patches; BM, bone marrow.

Supplemental items

Kober-Hasslacher-et-al_Supplemental-information-GCB_GSEA.xlsx

Kober-Hasslacher-et-al_Supplemental-information-RNASeq-DE-genes.xlsx

Kober-Hasslacher-et-al_Supplemental-information_cRel-nuclear-intensities.xlsx

Kober-Hasslacher-et-al_Supplemental-Methods.docx

Supplemental Methods

Antibodies used in flow cytometry

The following monoclonal antibodies against the indicated antigens were used:

eBioscience: AA4.1/CD93 (AA4.1), B220 (RA3-6B2), CD1d (1B1), CD4 (RM4-5), CD5 (53-7.3), CD8a (53-6.7), CD19 (1D3), CD21/CD35 (8D9), CD23/FcεRII (B3B4), CD25 (3C7, PC61.5), CD38 (90), CD43 (eBioR2/60), CD44 (IM7), CD62L (MEL-14), CD69 (H1-2F3), CD80 (16-10A1), CD86 (GL1), c-kit (2B8), c-Rel (1RELAH5), GL7 (GL7), ICOS/CD278 (7E.17G9), IgD (11-26c), IgG (11-4011), IgM (II/41), IRF4 (3E4), Ki-67 (SoIA15), MHC-II (M5/114.15.2), PD-1/CD279 (J43), TCRb (H57-597);

BD Biosciences: Bcl6 (K112-91), Blimp1 (5E7), CD95/Fas (Jo2), CXCR4/CD184 (2B11), CXCR5 (2G8), CD138 (281-2), CD21/CD35 (7G6), IgA (C10-1), IgE (R35-72), IgG1 (A85-1), IgG3 (R40-82), Igλ1 (R11-153);

BioLegend: B220 (RA3-6B2), CD4 (RM4-5), CD19 (6D5), CD38 (90), CD138 (281-2), TCRb (H57-597);

Miltenyi Biotec: c-Rel (REA397), flag (anti-DYKDDDDY monoclonal);

as well as well as antibodies against IgM (polyclonal, 115-126-075, Dianova) or staining with PNA (FL-1071, Vector Laboratories) or NP-PE (N-5070-1, Biosearch Technologies).

Western blot

For protein isolation, cells were lysed by incubation on ice in high salt lysis buffer (20 mM HEPES pH 7.9, 350 mM NaCl, 20% glycerol, 1 mM MgCl₂, 0.5 mM EDTA pH 8, 1% NP-40) containing 1 mM DTT, 1 mM PMSF, 5 mM NaF, 1 mM Na₃VO₄, 8 mM beta-glycerophosphate, 10 µg/µl leupeptin and 10 µg/µl aprotinin. Isolated protein sample separation by SDS-PAGE and blotting to PVDF membranes was followed by incubation with primary antibodies

against c-Rel (sc-71, Santa-Cruz Biotechnology) and tubulin (MAB1864, YL1/2, Millipore) as well as HRP-conjugated secondary antibodies (Dianova) to perform development using a chemiluminescent HRP substrate (Immobilon Western, Millipore).

Primary mouse cell culture for anti-CD40 activation

Splenocytes or MACS-purified B cells were cultured in RPMI1640 medium supplemented with 5% FCS, NEAA, sodium-pyruvate, HEPES, L-glutamine and penicillin/streptomycin (all Gibco). Anti-CD40 (HM40-3, eBioscience) was added at 4µg/ml. If indicated, the pancaspase inhibitor Q-VD-OPh (R&D Systems) was added to the culture medium to prolong survival of GCB cells in culture.

Immunofluorescence for GC quantification

For GC quantification, 7 µm sections were incubated with rat anti-Bcl6 antibody (7D1, Santa Cruz) at 4°C overnight and then incubated with donkey anti-rat IgG-AlexaFluor 594 (A21209, Invitrogen) together with DAPI for 1 h. Images were captured in Leica TSC SP8 confocal microscope with 40x optic with tilescan. The size of GCs was measured in ImageJ software.

FluoroSpot

Low auto-fluorescent 96-well polyvinylidene fluoride plates (Millipore) were pre-wetted with 25 µL 35% ethanol for no more than 1 min and immediately washed with sterile water three times (200 µL/well). Next, 100 µL/well NP-BSA (NP-2, NP-BSA ratio 1-4, Biosearchtech; or NP-23, NP-BSA ratio >20, Biosearchtech) diluted to 12.5 µg/mL in sterile PBS was incubated at 4 °C overnight. After washing three times with sterile PBS (200 µL/well), the wells were blocked with 200 µL/well culture medium (RPMI (Gibco) with 10% FCS (Gibco), 2mM L-glutamine (Gibco), 0.1 mM Non-essential amino acids (Gibco), 0.1% 2-Mercaptoethanol

(Gibco), 1 mM Na-Pyruvate (PAN-Biotech), 10 mM HEPES (Gibco), 1% Penicillin/Streptomycin (Gibco) for 1 hour at 37°C. Splenocytes were seeded at a density of 0.1, 0.4 and 1.6 Mio/ml, in 100 µL/well culture medium in duplicate wells. Cells were incubated overnight at 37 °C and 5% CO₂ and removed by washing the plates five times with PBS (200 µL/well). Detection antibodies, polyclonal AffiniPure goat-F(ab')₂ anti-mouse-IgM (µ chain)-PerCP (115-126-075, Jackson ImmunoResearch) and polyclonal AffiniPure goat Anti-Mouse IgG (Fcγ subclass 1)-Alexa Fluor 488 (115-545-205, Jackson ImmunoResearch) were diluted 1:500 in PBS containing 0.1% BSA (HyClone, GE Healthcare), and plates were incubated with 100µL/well for 2 h at room temperature. After washing five times with PBS (200 µL/well), 50 µL/well Fluorescence Enhancer-II (Mabtech) was incubated for 15 minutes at room temperature. The underdrain was removed and the plate left to dry, protected from light. Plates were sent to ImmunoSpot (Cellular Technology Limited, CTL) for readout, where fluorescent spots were detected using the ImmunoSpot S6 Ultra-V S6ULTRA Reader.

Quantification of immunofluorescence

2D quantification of 10 µm sections:

The code for quantification of nuclear c-Rel intensities of single B220⁺Bcl6⁻ mantle zone B cells and B220⁺Bcl6⁺ GC B cells is available below (Bcl6 staining: red, B220 staining: white). In brief, we applied the following steps. Step 1: We segmented the nucleus of the target staining image by using a machine learning-based interactive segmentation tool (1) and obtained the cell boundaries. Step 2: Since the initial mask contained a large amount of small noisy components, we performed connected component analysis to remove those small regions by defining an empirical threshold. We further used erosion operation to separate the neighboring masks and fill the holes in the masks. Thus, the masks of single

cells were well separated. Step 3: We quantified the nuclear intensities within single cells by using nuclear c-Rel staining (green) and Draq5 staining (blue) as the target cell nuclear masks. Specifically, we calculated the mean nuclear c-Rel intensities of individual cells after automatically labeling the separated cells using connected component analysis. Mantle zone B cells were defined as B220⁺Bcl6⁺ cells located outside the germinal center region defined by Bcl6 staining.

3D quantification of 30 μm sections:

3D Image analysis of 30μm sections was performed using Imaris software (Bitplane) on maximum projections of 10 Z-plane sections following adaptive image deconvolution using the LIGHTNING tool (Leica). Automated analyses using the Imaris surface generation tool was used for cell identification and segmentation based on B220 and Bcl6 staining. Mantle zone B cells and GC B cells were defined as described above. Generation of individual surface objects for cell nuclei was done using nuclear DRAQ5 staining. For histocytometric analysis, statistics for mean voxel intensities for fluorescence channels and positional information for surface objects were exported into Excel (Microsoft) and plotted in FlowJo software (TreeStar Inc) after conversion into CSV files.

Codes in Python for immunofluorescence image quantification

```
import os
import numpy as np
import matplotlib.image as mpimg
import cv2
import scipy.ndimage.measurements as measurements
from scipy import ndimage

#### read tiff images and masks
ID = '*your target image*' #your target image
intensity_G_Nu_nonRed_single = []
intensity_G_Nu_Red_single = []
result_dir = 'result_'+ID+'/'
mask_dir = data_dir+ID+'masks'+ '/' # where the cell masks locate
```



```

raw_dir = data_dir+ID+'_rawfiles/' # where the raw files locate
if not os.path.exists(result_dir):
    os.makedirs(result_dir)
blue_mask = np.load(mask_dir+ID+'blue.npy') # read the masks of one type of cells
red_mask = np.load(mask_dir+ID+'red.npy') # read the masks of another type of cells

blue_mask = blue_mask[...0]
blue_mask.setflags(write=1)
blue_mask[blue_mask == 1] = 0 #reset the labels from the original files, background = 0
blue_mask[blue_mask == 2] = 1

mpimg.imsave(result_dir+"blue_mask.png", blue_mask*255)

red_mask = red_mask[...0]
red_mask.setflags(write=1)
red_mask[red_mask == 1] = 0
red_mask[red_mask == 2] = 1
red_mask = np.uint8(red_mask)
mpimg.imsave(result_dir+"red_mask.png", red_mask*255)

##### preprocessing the masks
#find all the connected components (white blobs in your image)
nb_components, output, stats, centroids = cv2.connectedComponentsWithStats(blue_mask,
connectivity=8)
#connectedComponentsWithStats yields every separated component with information on
each of them, such as size
#the following part is just removing the noisy background, which is also considered a
component, but most of the time we don't want that.
sizes = stats[1:, -1]; nb_components = nb_components - 1
# minimum size of particles we want to keep (number of pixels)
#here, it's a fixed value, but you can set it as you want, e.g. the mean of the sizes or
whatever
min_size = 250

pre_blue_mask = np.zeros((output.shape))
#for every component in the image, you keep it only if it's above min_size
for i in range(0, nb_components):
    if sizes[i] >= min_size:
        pre_blue_mask[output == i + 1] = 1
kernel = np.ones((2,2),np.uint8)
erosion = cv2.erode(np.uint8(pre_blue_mask),kernel,iterations = 1)
erosion = ndimage.binary_fill_holes(erosion).astype(int)

# another round of selection, removing small components
pre_blue_mask_ = np.zeros((output.shape))
nb_components, output, stats, centroids =
cv2.connectedComponentsWithStats(np.uint8(erosion), connectivity=8)
sizes = stats[1:, -1]; nb_components = nb_components - 1

```

```

for i in range(0, nb_components):
    if sizes[i] >= min_size:
        pre_blue_mask_[output == i + 1] = 1

mpimg.imsave(result_dir+"pred_blue_mask_erosion.png", pre_blue_mask_*255)
mpimg.imsave(result_dir+"pre_blue_mask.png", pre_blue_mask*255)

nb_components, output, stats, centroids =
cv2.connectedComponentsWithStats(np.uint8(red_mask), connectivity=4)
sizes = stats[1:, -1]; nb_components = nb_components - 1
min_size = 300
pre_red_mask = np.zeros((output.shape))
#for every component in the image, you keep it only if it's above min_size
for i in range(0, nb_components):
    if sizes[i] >= min_size:
        pre_red_mask[output == i + 1] = 255

pre_red_mask = ndimage.binary_fill_holes(pre_red_mask).astype(int)
mpimg.imsave(result_dir+"pre_red_mask.png", pre_red_mask*255)
mass_red = ndimage.binary_fill_holes(pre_red_mask).astype(int)
centerOfMass = measurements.center_of_mass(mass_red)
radius = np.sum(mass_red)
mass_red = np.zeros_like(pre_red_mask)
for ii in range(np.shape(pre_red_mask)[0]):
    for jj in range(np.shape(pre_red_mask)[1]):
        if (ii-centerOfMass[0])*(ii-centerOfMass[0])+(jj-centerOfMass[1])*(jj-
centerOfMass[1])<radius:
            mass_red[ii, jj] = 1
mpimg.imsave(result_dir+"mass_red.png", mass_red*255)
mpimg.imsave(result_dir+"mass_NonRed.png", (1-mass_red)*255)

####quantification of the green staining intensities of one type of cells
green = mpimg.imread(raw_dir+"ch03.tif") # the image name of the green staining
region_red_cell = mass_red[...]*pre_blue_mask_[...]*pre_red_mask[...]
region_red_cell_selected = np.zeros((output.shape))
nb_components, output, stats, centroids =
cv2.connectedComponentsWithStats(np.uint8(region_red_cell), connectivity=8)
sizes = stats[1:, -1]; nb_components = nb_components - 1

for i in range(0, nb_components): # quantification of each cell
    if sizes[i] >= min_size:
        region_red_cell_selected[output == i + 1] = 1
        intensity_G_Nu_Red_single.append(np.mean(green[output == i + 1, 1]))
    if i == nb_components-1:
        intensity_G_Nu_Red.append(intensity_G_Nu_Red_single)
mpimg.imsave(result_dir+"Red_nucleus.png", region_red_cell_selected*255)

####quantification of the green staining intensities of another type of cells

```

```
region_non_red_cell = (1-mass_red)[...]*pre_blue_mask_[...]*(1-pre_red_mask)[...]  
region_non_red_cell_selected = np.zeros((output.shape))  
nb_components, output, stats, centroids =  
cv2.connectedComponentsWithStats(np.uint8(region_non_red_cell), connectivity=8)  
sizes = stats[1:, -1]; nb_components = nb_components - 1  
for i in range(0, nb_components):  
    if sizes[i] >= min_size:  
        region_non_red_cell_selected[output == i + 1] = 1  
        intensity_G_Nu_nonRed_single.append(np.mean(green[output == i + 1, 1]))  
    if i == nb_components-1:  
        intensity_G_Nu_nonRed.append(intensity_G_Nu_nonRed_single)  
mpimg.imsave(result_dir+"non_Red_nucleus.png", region_non_red_cell_selected*255)
```

Reference

1. Sommer C, Straehle C, Kothe U, Hamprecht FA. ilastik: Interactive Learning and Segmentation Toolkit. Eighth IEEE International Symposium on Biomedical Imaging (ISBI), Proceedings 2011:230–233.